Pin Design for Part Feeding

Tao Zhang[=] Ken Goldberg[*] Gordon Smith[Γ]
Robert-Paul Berretty[♦] Mark Overmars[↔]

[=]Dept. of Industrial Eng.
& Operations Research,
University of California at Berkeley,
Berkeley, CA 94720-1777 USA

[*]Dept. of Industrial Eng. & Operations Research,
and Dept. of Electrical Eng. & Operations Research,
University of California at Berkeley,
Berkeley, CA 94720-1777 USA

[Γ]Dept. of Mechanical Eng.,
University of California at Berkeley,
Berkeley, CA 94720-1740 USA

[♦]Department of Computer Science,
University of North Carolina at Chapel Hill,
Campus Box 3175, Sitterson Hall,
Chapel Hill, NC 27599-3175, USA

[↔]Dept. of Computer Science,
Utrecht University,
3508 TB Utrecht, The Netherlands

Abstract-- We consider a sensorless approach to feeding parts on a conveyor belt using pins (rigid barriers) to topple parts into desired orientations. Given the *n*-sided 2D convex projection of an extruded polygonal part, its center of mass (COM), and coefficients of friction, we develop an $O(n^2)$ algorithm to compute the *toppling graph*, a new data structure that represents the mechanics of toppling including rolling and jamming. The toppling graph can be used to identify critical pin heights that permit toppling. We compare pin heights predicted by the graph with physical experiments, and give a complete $O(n^{3n})$ algorithm for designing pin sequences.

Index Terms-- Robotics, Parts feeding, Planning, Toppling manipulation.

I. INTRODUCTION

There is a growing demand for automated manipulation analysis, especially efficient algorithms, for modern manufacturing. Efficient algorithms can be incorporated to commercial CAD/CAM software packages to facilitate rapid setup and changeover of assembly lines.

Lynch[1,2] analyzes how a part can be toppled by programmable pins to a new orientation as it moves on a conveyor belt. In this paper we extend his analysis with a geometric algorithm for designing fixed pin sequences for part feeding.

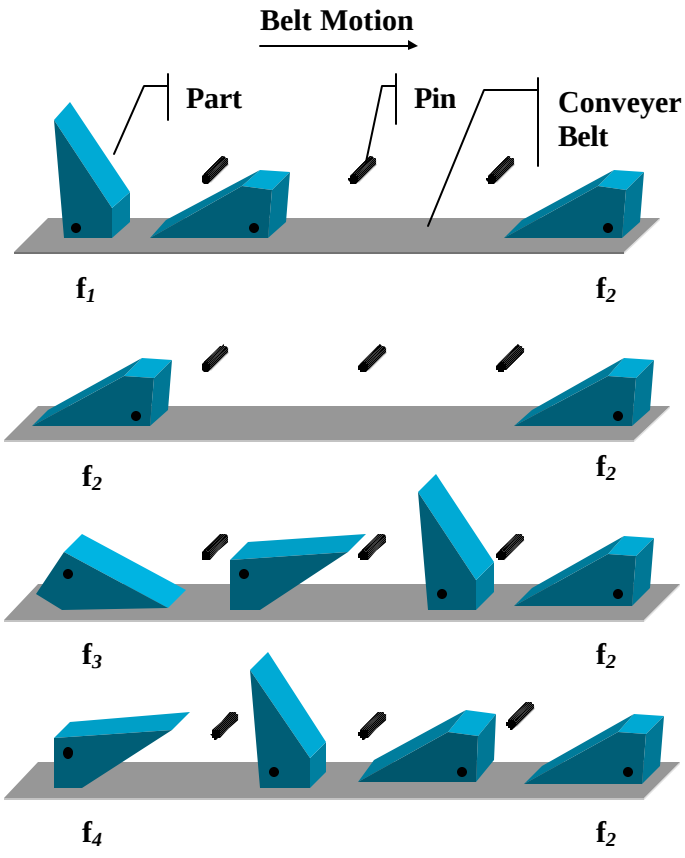

Figure 1. The sequence of 3 pins will orient the part as it moves from left to right: four different initial part orientations reach orientation f_2.

Given the *n*-sided 2D convex projection of an extruded polygonal part, its center of mass, and coefficients of friction, we want to find a sequence of the pins (if exists) such that the part emerges in a unique final orientation after moving through. The first step is to find the critical pin heights at each of the part's stable orientation where the pin can topple the part from one stable orientation to the next; the second step is to solve a planing problem to design an arrangement of the pins.

Our analysis involves the graphical construction of a set of functions that represent the mechanics of toppling. All these functions map from part orientation to distance: $\boldsymbol{S}^1 \rightarrow \hat{\mathbf{A}}^+$, where $\boldsymbol{S}^1$ is the set of planar orientations. We name them *shape functions*. The *toppling graph* is a new data structure that combines shape functions to help us to identify the critical pin heights.

II. RELATED WORK

Erdmann and Mason[3] introduce a systematic algorithm for sensorless manipulation to orient parts using a tilting tray. Brost[4] develops dynamic analytical methods for describing the interaction between a pair of polygonal objects in the configuration-space (C-space), and gives algorithms for constructing a set of initial configurations from which a given operation will accomplish a set of goal configuration in the presence of uncertainty. Goldberg[5] demonstrates that a sequence of normal pushes can orient polygons up to symmetry. Abell and Erdmann[6] study how a planar polygon can be rotated in a gravitational field while stably supported by two frictionless contacts. Zumel and Erdmann[7,8] analyze nonprehensile manipulation using two palms jointed at a central hinge and also develop a sensorless approach to orient parts.

Lozano-Perez[9] studies the design of part feeding devices as a dual to motion planning. He applied C-space diagram to describe the function of the devices. The limitation of this approach is that the legal position of the maximal feeders and the swept volumes are dependent on each

other. Therefore, a generate-and-test paradigm has to be used to for the candidates. In this paper, we develop a different C-space model based on the mechanics of pins. Natarajan[10] focus on a computational abstraction for part-feeding devices using flow network analysis. Given k transfer functions, $f_1, f_2, \ldots, f_k$, on a finite set $\boldsymbol{S}$, Natarajan shows that f_0, if it exists, can be found in time $O(kn^4)$ such that $|f_0(\boldsymbol{S})| = |\{f_0(v) \mid v \in \boldsymbol{S}\}| = 1$, where f_0 is a composite of the f_i's and n is the size of $\boldsymbol{S}$. Caine[11] represents part interactions as motion constraints in C-space, and develop a set of computational tools to design vibratory bowl feeder tracks. Christiansen *et al.*[12] utilize genetic algorithms to the design of vibratory feeder tracks; and Berkowitz and Canny[13] apply dynamic simulation to design part-feeding devices which allowed the user to easily generate and test the feeders.

Conveyor belts with rigid fences are initially analyzed by Peshkin and Sanderson[14], who develop a numeric search algorithm to find the sequence of the fences to orient parts based on C-space analysis. Wiegley *et al.*[15] give a complete algorithm to compute the shortest sequence of frictionless curved fences, and Berretty *et al.*[16] propose a polynomial-time algorithm to find such a sequence for any polygonal part. Gudmundsson and Goldberg[17] derive the optimal belt velocity of a part feeder based upon a 1D Poisson process model. Akella *et al.*[18] consider a minimalist manipulation method to feed planar parts using a one joint robot over a conveyor belt.

Many other part feeding devices have been studied. Bicchi and Sorrentino[19] analyze the mechanics of rolling with a pair of parallel jaws. Berretty *et al.*[20] study traps and give algorithms to decide whether or not the part in a specific orientation will fall into a trap under the influence of gravity. Blind *et al.*[21] invent a "*Pachinko*"-like device to orient polygonal parts in

the vertical plane. It consists of a grid of retractable pins that are programmed to bring the part to a desired orientation as the part falls.

Our work is also motivated by recent research in toppling manipulation. Zhang and Gupta[22] study how parts can be reoriented as they fall down a series of steps. The authors derive the condition for toppling over a step and define the transition height, which is the minimum step height to topple a part from a given stable orientation to another. Yu *et al.*[23] estimate the mass and COM of objects by toppling. Lynch[1,2] derives sufficient mechanical conditions for toppling parts on a conveyor belt in term of constraints on contact friction, location, and motion.

III. Problem Definition

We assume that pins are fixed and rigid, inertial forces are negligible, and that part geometry and location of its COM are known exactly.

The input of our algorithm is a 2D projection of an n-sided convex part, its COM, μ_t and μ_p: the part-track friction coefficient and the part-pin friction coefficient. The output of our algorithm is a (possibly empty) range of critical pin heights for the part at each stable orientation. A pin at a critical pin height can topple the part from that stable orientation to the next.

Figure 2 shows the notation used in our toppling analysis on a 2D projection of a part. The part moves from left to right on the conveyor belt. The conveyor friction cone half-angle is $\alpha_t = \tan^{-1}\mu_t$ and the pin friction cone half-angle is $\alpha_p = \tan^{-1}\mu_p$. The pivot point is the vertex about which the part rotates and taken to be at (0,0). The COM is a distance r from the origin and an angle θ from the +X axis at an initial stable orientation. We denote the vector at the left edge of the pin's friction cone as f_l and the right edge as f_r.

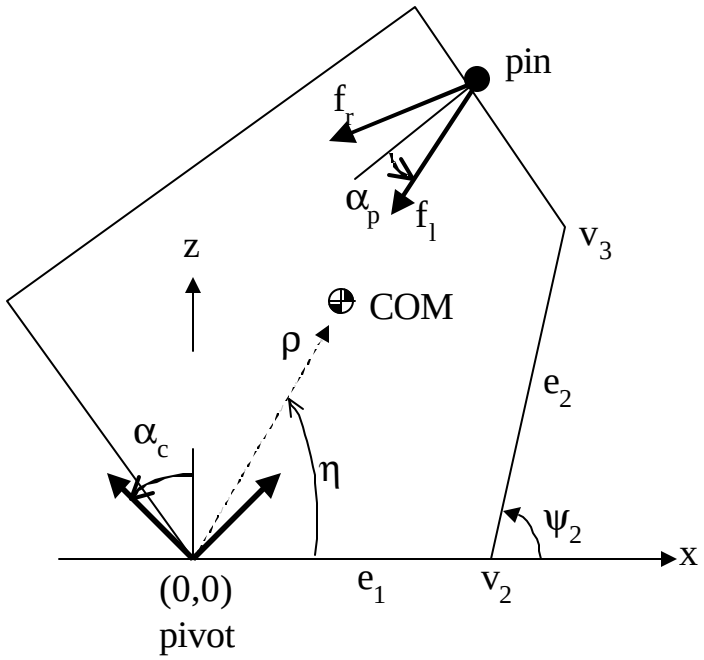

Figure 2. Notation.

Starting from the pivot, we consider each edge of the part in counter-clockwise order, namely e_1, e_2, …, e_n. The edge e_i, with vertices v_i at (x_i, z_i) and v_{i+1} at (x_{i+1}, z_{i+1}), is in direction γ_i from the +X axis. The analysis given below is repeated for each stable orientation of the part.

IV. TOPPLING ANALYSIS

We divide toppling into a rolling phase and a settling phase as shown in Figure 3. Let θ denote the orientation of the part from the +X axis. *Rolling* involves the rotation of the part from the initial orientation ($\theta = \theta_0$) to the unstable equilibrium orientation ($\theta = \theta_t$) where the COM is directly above the pivot. During *Settling*, the part rotates from the unstable equilibrium orientation to the next stable orientation ($\theta = \theta_n$).

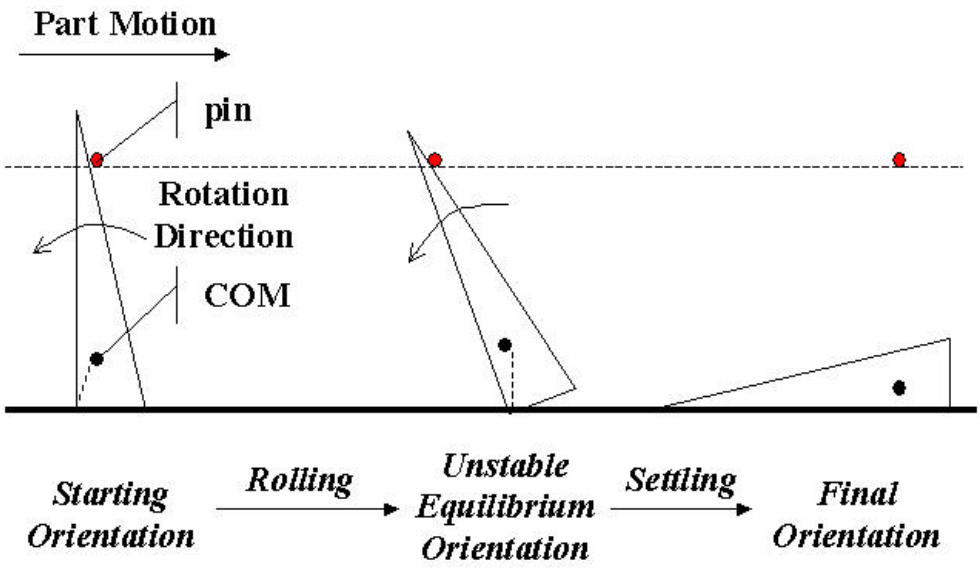

Figure 3. Two phases of toppling.

The radius function, $R(\theta)$, indicates the height of the COM as the part rotates; the vertex height function, $V_i(\theta)$, describes the height of vertex i, which is visible from +X axis, as the part rotates; the rolling height function, $H_i(\theta)$, is determined for each edge at $\theta_0 < \theta < \theta_t$; the jamming height function, $J_i(\theta)$, is determined for each edge at $\theta_t < \theta < \theta_n$. All four of these functions are combined to form the toppling graph from which we can determine the critical pin heights for the part.

A. Radius Function

The radius function R: $S^1 \rightarrow \hat{\mathbf{A}}^+$, gives the height of COM as the part rotates. Each local minimum of the function corresponds to a stable orientation of the part[5]. Note that a pin at a height h contacts edge e_i if $V_i(\theta) < h < V_{i+1}(\theta)$.

B. Vertex Height Functions

The vertex height function, $V_i(\theta) = x_i \sin\theta + z_i \cos\theta$, describes the height of vertex i as the part rotates. Like the radius function, it is piecewise sinusoidal. The vertex height function is truncated after its global maximum at the point where it intersects another vertex height function. This is the point at which the vertex is no longer visible from the +X axis and therefore can no longer be contacted by a pin. Figure 4 illustrates the vertex height functions and the radius function for the part in Figure 2.

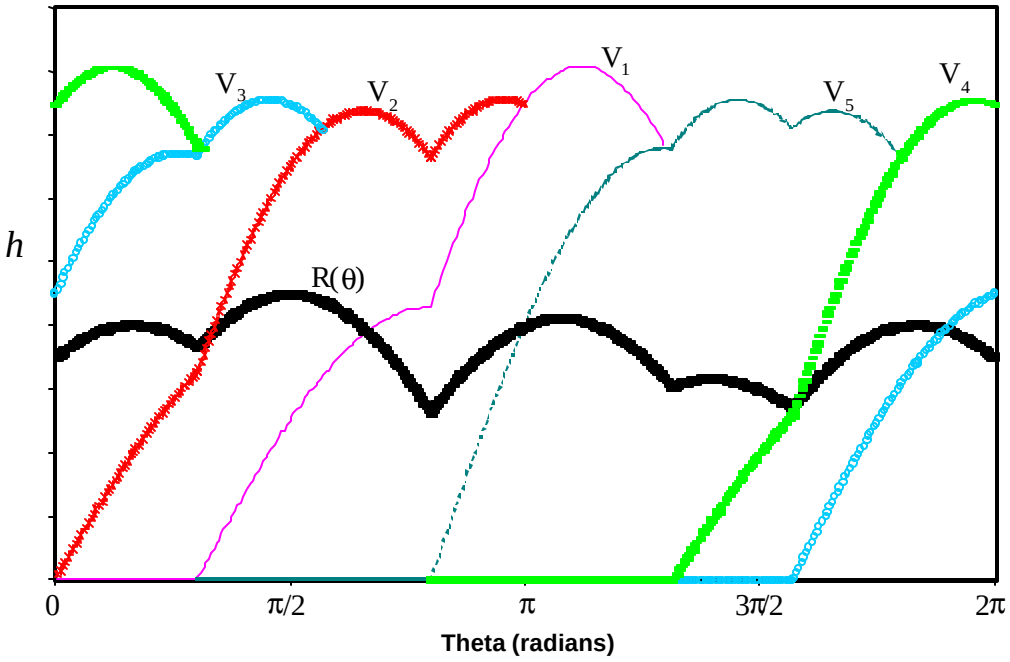

Figure 4. Radius function, $R(\theta)$, and vertex height functions, $V_i(\theta)$.

C. Rolling Height Functions

During rolling, the part rotates about the pivot point. Friction between the part and the conveyor belt must prevent the pivot point from sliding relative to the belt; but friction between the part and the pin must not prevent the part from slipping relative to the pin. Additionally, the system of forces on the part: the contact force at the conveyor, the contact force at the pin, and

the part's weight, must generate a positive (counterclockwise) moment on the part about the pivot point.

The rolling height function, $H_i(\theta)$, is the minimum height that the toppling contact in edge e_i must be in order to roll the part during the rolling process, where $\theta = \theta_0 \sim \theta_1$. The function is determined as a function of θ using an analysis adapted from the rolling conditions in Lynch[1]. Those conditions are derived using a graphical method from Mason[24].

We begin by constructing a region as shown in Figure 5 with vertices P_1 at ($r\cos(\eta+\theta)$, $r\cos(\eta+\theta)/m_t$), P_2 at (0,0), and P_3 at ($r\cos(\eta+\theta)$, $-r\cos(\eta+\theta)/m_t$). For a fixed pin to cause rolling, the contact force between the pin and the part must make positive moment about every point in the $P_1P_2P_3$ triangle.

Additionally, by examining the kinematics of the part and the pin during rotation, we can determine which direction the pin slips relative to the part. This knowledge allows us to limit our consideration to one edge of the friction cone, depending on the direction of slip. In general, the rolling conditions will depend on whether the contact has a positive or negative X coordinate, i.e. whether it is right or left of the Z-axis.

Let w_i be the distance along edge e_i as shown in Figure 5. Any point on e_i can be expressed in terms of w_i as $(x_i + w_i \cos\gamma_i, y_i + w_i \sin\gamma_i)$. Let w_i^* denote the critical w_i where the contact is on the Z-axis. Therefore, we have:

$$x_i \cos\theta - z_i \sin\theta + w_i^* \cos(\gamma_i + \theta) = 0,$$

or

$$w_i^* = (-x_i \cos\theta + z_i \sin\theta)/\cos(\gamma_i + \theta), \qquad (1)$$

and the height of the point at w_i^* is:

$$H_i^*(\theta) = x_i \sin\theta + z_i \cos\theta + w_i^* \sin(\gamma_i + \theta). \quad (2)$$

The contact is left of the Z-axis if $w_i > w_i^*$; right of the Z-axis if $w_i > w_i^*$. Let $H_{il}(\theta)$ denote $H(\theta)$ when the contact is left of the Z-axis, and $H_{ir}(\theta)$ denote $H(\theta)$ when the contact is right of the Z-axis.

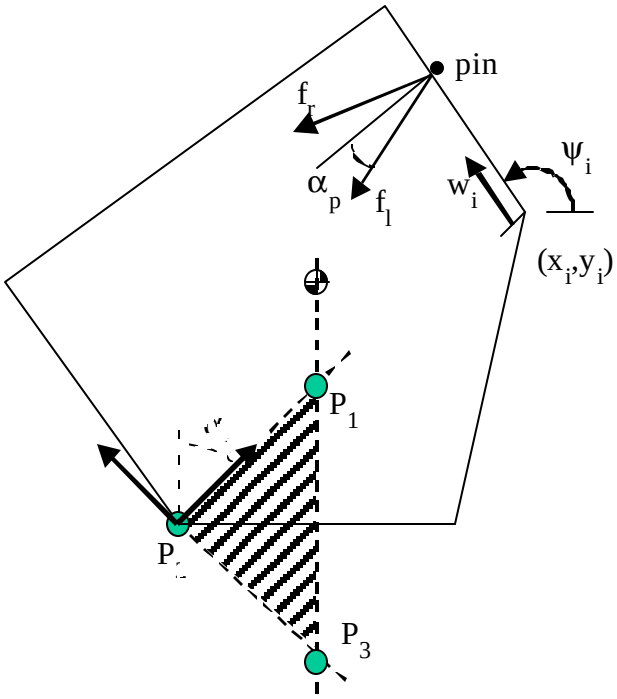

Figure 5. Rolling condition.

1) Contact to the right of the Z*-axis*

For the case where $w_i \le w_i^*$, as the part rotates, the contact between the part and the pin moves such that w_i is decreasing. Therefore, the contact force must be at the left edge of the pin friction cone. The rolling height for this case is determined by projecting lines from P_1 and P_2 at

the angle of f_l until they intersect the edge of the part. Of these two intersections, the one with the maximum height indicates the rolling height, $H_{il}(\theta)$, if it is less than $H_i^*(\theta)$.

Let ${}_1w_{il}(\theta)$ denote the pin contact on e_i where f_l passes exactly through point P_1. We can show through geometric construction that:

$$ {}_1w_{il}(\theta) = (2m_t z_i \cos\beta_{il} - r\cos(\beta_{il}-\eta) - r\cos\nu_{il} - 2m_t x_i \sin\beta_{il} + m_t r\sin(\beta_{il}-\eta) + m_t r\sin\nu_{il}) / (2m_t \sin(\beta_{il}-\gamma_i)). \quad (3) $$

where $\beta_{il} = \gamma_i + \pi/2 + \alpha_p$ and $\nu_{il} = \beta_{il} + \eta + 2\theta$.

Similarly, the contact on e_i for f_l passing through P_2 is given by

$$ {}_2w_{il}(\theta) = (z_i\cos\beta_{il} - x_i\sin\beta_{il}) / \sin(\beta_{il}-\gamma_i). \quad (4) $$

Let $w_{il}^{\#}$ denote the maximum of ${}_1w_{il}$ and ${}_2w_{il}$. By geometry, $w_{il}^{\#}$ can be shown to be

$$ w_{il}^{\#} = \begin{cases} {}_1w_{il} & 0 < \theta < \theta_{12} \\ {}_2w_{il} & \theta_{12} < \theta < \theta_2 \end{cases} \quad (5) $$

where

$$ \theta_{12} = \pi - \alpha_t - \alpha_p - \gamma_i \quad (6) $$

$$ \theta_2 = \pi - \alpha_p - \gamma_i \quad (7) $$

Therefore, for $w_i \le w_i^*$, the rolling height function, $H_{il}(\theta)$ is given by

$$H_{il}(\theta) = x_i \sin\theta + z_i \cos\theta + w_{il} \sin(\gamma_i + \theta), \tag{8}$$

where

$$w_{il} = \begin{cases} 0 & w_{il}^{\#} < 0 \\ w_{il}^{\#} & 0 \le w_{il}^{\#} \le w_i^{*} \\ w_i^{*} & w_{il}^{\#} > w_i^{*} \end{cases}. \tag{9}$$

2) Contact to the left of the Z*-axis*

In this case, where $w_i > w_i^{*}$, the contact between the part and the pin moves such that w_i is increasing. Therefore, the contact force must be at the right edge of the pin friction cone. Rolling is guaranteed if a force at the angle of the right edge of the pin friction cone generates a positive moments about the $P_1P_2P_3$ triangle.

Let ${}_1w_{ir}(\theta)$ denote the contact on e_i where f_i passes exactly through point P_1. We can show through geometric construction that:

$${}_1w_{ir}(\theta) = (2\mu_t z_i \cos\beta_{ir} - r\cos(\beta_{ir}-\eta) - r\cos\nu_{ir} - 2\mu_t x_i \sin\beta_{ir} + \mu_t r\sin(\beta_{ir}-\eta) + \mu_t r\sin\nu_{ir}) / (2\mu_t \sin(\beta_{ir} - \gamma_i)). \tag{10}$$

where $\beta_{ir} = \gamma_i + \pi/2 - \alpha_p$ and $v_{ir} = \beta_{ir} + \eta + 2\theta$.

There is no angle at which a force at f_i will pass through P_1 or P_3 and be higher than ${}_2w_{ir}(\theta)$. Therefore, for $w_i > w_i^{*}$, $H_{ir}(\theta)$ is given by:

$$H_{ir}(\theta) = x_i \sin\theta + z_i \cos\theta + w_{ir} \sin(\gamma_i + \theta), \tag{11}$$

where

$$w_{ir} = \begin{cases} w_i^* & {}_1w_{ir} \le w_i^* \\ {}_1w_{ir} & w_i^* \le {}_1w_{ir} \le l_i \\ \infty & {}_1w_{ir} \ge l_i \end{cases} \qquad (12)$$

and l_i is the length of edge e_i.

3) Contact on both sides of the Z-axis

Note that if an edge has part of its length to the left of the Z-axis and part right of the Z-axis, there may be two separated contact regions on the edge where rolling can occur. For this reason there will be three rolling height functions: $H_{il}(\theta)$ for the partial edge left of the Z-axis, $H_{ir}(\theta)$ for the partial edge right of the Z-axis, and $H_i^*(\theta)$. For this case, the pin at height h can roll the part if $H_i^*(\theta) > h > H_{ir}(\theta)$ or $h > H_{il}(\theta)$, where $\theta_t < \theta < \theta_t$.

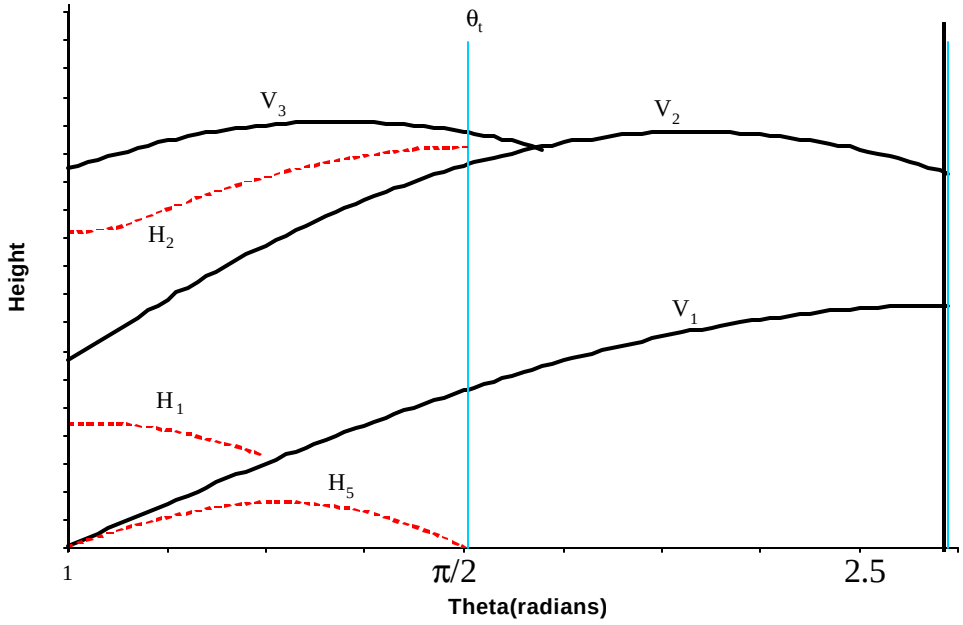

Figure 6. The functions $H_{il}(\theta)$, $H_{ir}(\theta)$, and $H^*(\theta)$.

Figure 6 illustrates the functions $H_i(\boldsymbol{q})$ where the pivot is v_5 in Figure 2. In this case α_t = 0.65cm, $\boldsymbol{a}_p$ = 0.09cm, $\boldsymbol{r}$ = 9cm, and $\boldsymbol{h}$ = 50°. The kink in $H_2(\boldsymbol{q})$ indicates the rotational angle where ${}_2w_{2r}$ becomes higher than ${}_2w_{1r}$. We determine $H_i(\boldsymbol{q})$ for each visible edge of the stable orientations. Note that $H_i(\boldsymbol{q})$ must be bounded by the $V_i(\boldsymbol{q})$ and $V_{i+1}(\boldsymbol{q})$ and is truncated where it intersects those functions.

D. Jamming Height Function

After the part has rotated to $\boldsymbol{q}_t$, rolling process ends and settling starts. The part may jam while settling due to the friction. We intend to determine if the part will fall to the next stable orientation. Note that we do not consider the full dynamics of the settling process or allow the part to rotate past the next stable orientation due to its momentum.

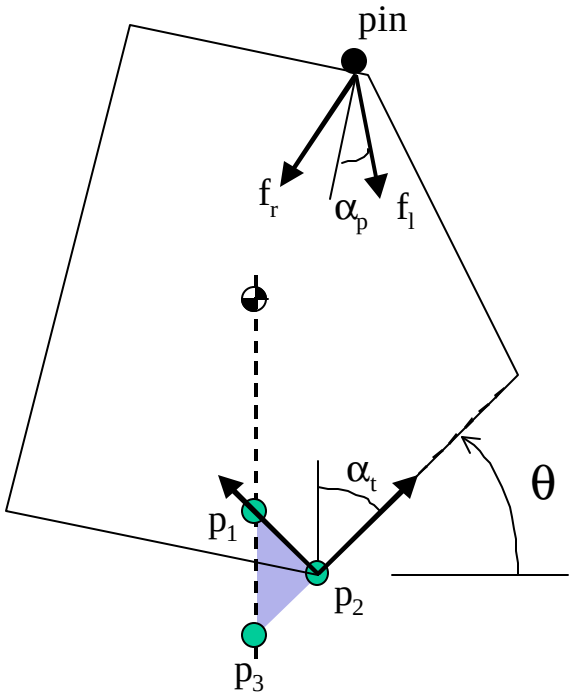

Figure 7. Jamming condition.

Jamming is the compliment of the rolling process. For rolling all forces within the pin friction cone must make a positive moment about the $P_1P_2P_3$ triangle; to guarantee no jamming any force within the pin friction cone must not make a negative moment about $P_1P_2P_3$. Figure 7 shows that due to the position of the COM during settling the $P_1P_2P_3$ triangle is oriented in the opposite direction as during rolling. Therefore, we again divide our consideration into the situations where the contact is at the left/right of Z-axis.

1) Contact to the right of the Z-axis

When the contact is right of the Z-axis, rotation causes the contact to move such that w_i is decreasing. The contact force, therefore, is at f_1. Projecting lines at the angle of the left edge of the friction cone from P_1, P_2, and P_3 until they intersect the edge, we obtain:

$$ {}_3w_{il}(\theta) = (2m_t z_i \cos\beta_{il} + r\cos(\beta_{il}-\eta) + r\cos\nu_{il} - 2m_t x_i \sin\beta_{il} + m_t r\sin(\beta_{il}-\eta) + m_t r\sin\nu_{il}) / (2m_t \sin(\beta_{il}-\gamma_i)). \quad (13) $$

Any pin lower than the minimum of these three functions will cause jamming. Let $q_{il}^{\#}$ be the minimum of ${}_1w_{il}$, ${}_2w_{il}$, and ${}_3w_{il}$. $q_{il}^{\#}$ can be shown to be

$$ q_{il}^{\#} = \begin{cases} {}_3w_{il} & q_t < q < q_{32} \\ {}_2w_{il} & q_{32} < q < q_{21} \\ {}_1w_{il} & q_{21} < q < p - \gamma \end{cases} \quad (14) $$

where

$$ q_{21} = p + \alpha_t - \alpha_p - \gamma_i \quad (15) $$

$$\theta_{32} = \pi - \alpha_t - \alpha_p - \gamma_i \tag{16}$$

Therefore, The jamming height function for this situation, $J_{il}(\theta)$, is then given by

$$J_{il}(\theta) = x_i \sin\theta + z_i \cos\theta + q_{il} \sin(\gamma_i + \theta) \tag{17}$$

where

$$q_{il} = \begin{cases} 0 & q_{il}^{\#} \le 0 \\ q_{il}^{\#} & 0 \le q_{il}^{\#} \le w_i^* \\ w_i^* & q_{il}^{\#} > w_i^* \end{cases} \tag{18}$$

and $\theta_t < \theta < \theta_n$.

2) Contact to the left of the Z-axis

When the contact is left of the *Z*-axis, rotation causes the contact to move such that w_i is increasing. The contact force, if exists, is at f_r. In this situation it is impossible to cause jamming since f_r cannot create a negative moment about the $P_1P_2P_3$ triangle. Therefore the jamming height function equals 0, i.e., $J_{ir}(\theta) = 0$, when $w_i > w_i^*$,

E. The Toppling Graph

Figure 8 illustrates the entire toppling graph that combines the radius, vertex height, rolling height, and jamming height functions to represent the full mechanics of toppling. From the toppling graph the critical pin heights for each visible edge of each stable orientation can be determined or shown to be non-existent.

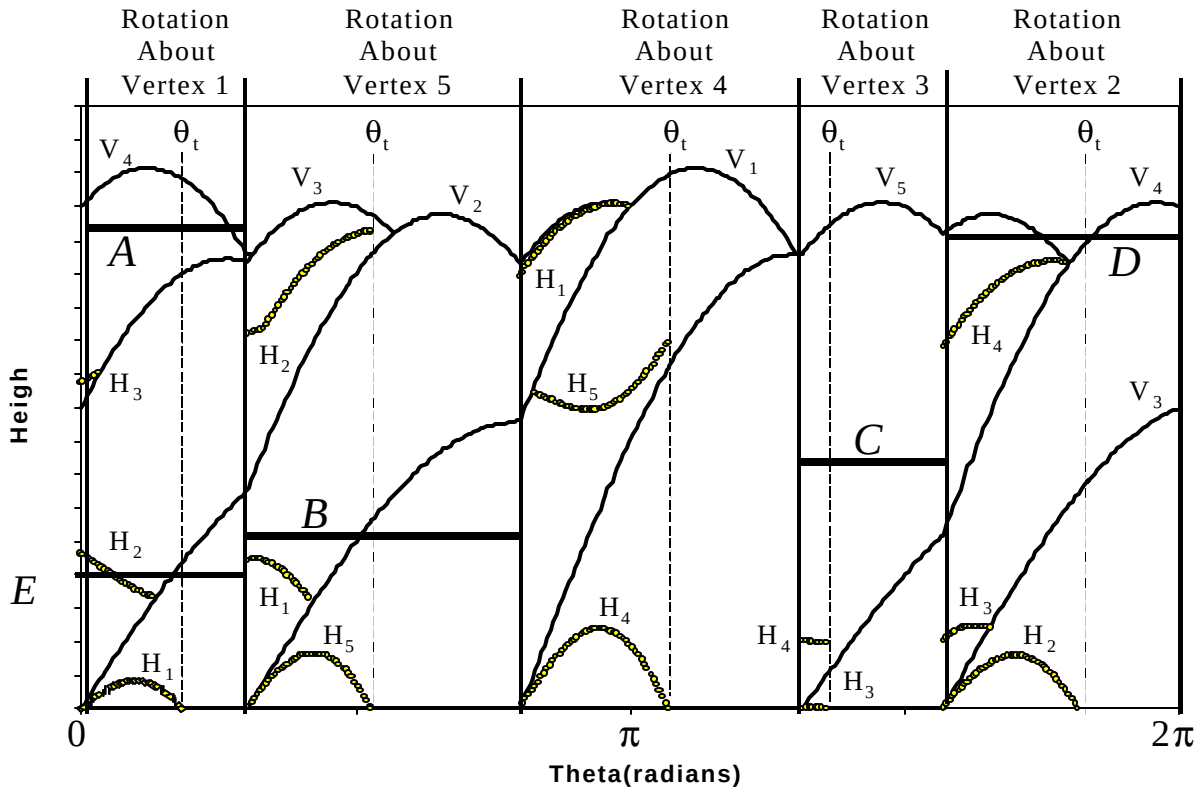

Figure 8. The toppling graph for the part in Figure 2.

For toppling from one stable orientation to the next to be successful there must exist a horizontal line from the angle of the stable orientation to the angle of the next stable orientation at height h that has the following characteristics:

1. if $V_i(\theta) < h < V_{i+1}(\theta)$, then $H_i^*(\theta) > h > H_{ir}(\theta)$ or $h > H_{il}(\theta)$, where $\theta_l < \theta < \theta_t$;

2. if $V_i(\theta) < h < V_{i+1}(\theta)$, then $J_{il}(\theta) < h$, where $\theta_l < \theta < \theta_n$; and

3: $h < \max_i (V_i(\theta))$, where $\theta_l < \theta < \theta_t$.

The first two criteria are satisfied when the pin is above both the rolling height and the jamming height on the edge it contacts. When h crosses a vertex height function, the part switches contact edges and then h must be above the rolling height and jamming height functions for the new edge. The third criterion is that the pin must not lose contact with the part by passing over it during the rolling phase.

Note on the graph that the solid vertical lines indicate the angles of stable orientations and the dashed vertical lines indicate θ_i's. From the graph we can determine a range of heights for each stable orientation in which a pin will topple the part to the next stable orientation, or determine the range does not exist.

The toppling graph described above predicts for each orientation of the part the *immediate action function* that takes place when the part hits a pin at a specified height. The four possible values of the function are:

- *Non-action*: the part passes under the pin or hits the pin but falls back to the same stable orientation;
- *Jamming*: the part gets stuck;
- *Repeating*: the part turns to the next stable orientation and will hit the same pin again;
- *Passing*: the part turns to the next stable orientation and will not hit the same pin again.

For example a pin at height A will cause Passing; while at B and C Repeating will occur. Note that B switches edges during rotation. D is an example of Non-action, where rotation begins but is not successful due to loss of contact with the part before reaching θ_1. E represents Jamming when the pin contacts with edge e_2.

V. PHYSICAL EXPERIMENTS

We conducted physical experiments using an Adept Flex Feeder conveyor belt. The part from Figure 2 was machined from aluminum and the pin from steel. The corresponding friction cone half angles are $\alpha_t = 53° \pm 2°$ (the belt is made from a high friction material), and $\alpha_p = 5° \pm 2°$. The critical pin heights predicted by the toppling graph and measured with physical experiments are compared in Table 1.

Pivot Vertex	Initial Contact Edge	Critical Pin Heights (cm)	
		Prediction	Experiment
1	2	[2.9, 5.7]	[2.8, 5.7]
1	3	[8.3, 9.5]	[8.3, 9.5]
5	1	[2.6, 4.1]	[2.6, 4.1]
3	4	[1.2, 8.6]	[1.8, 8.6]
2	3	[1.5, 3.4]	[1.5, 3.4]

Table 1. Comparison of prediction with experiment.

Although our friction measurements are inexact, the predictions are close in all cases except the lower bound in row 4. Since we project w_i onto the vertical to find $H_i(\theta)$, errors along the edge are projected and thus reduced by the sine of the edge angle. The sine is close to 1 in the 4^{th} row, thus this error is larger. For the upper bounds in this row, the top of the edge defines the limit in both prediction and experiment.

VI. PIN PLANNING

We want to use the toppling graph to design a sequence of pins such that a part will turn from an initial unknown orientation into a unique final orientation, if possible.

To this end, for each stable orientation, we want to compute the immediate action function. This function maps the height of the pin to four possible values: Non-action, Jamming, Passing, and Repeating. We can easily extract this information from the toppling graph. The complexity of the immediate action function is the same as the complexity of the toppling graph: for each of the $O(n)$ stable orientations of the part, there are $O(n)$ possible intervals linked to actions.

Rather than the immediate action, we would like to know what the final outcome will be after the part interacts with a pin. Therefore we define the *final outcome function* for each stable orientation. This function maps a pin height to the index of a stable orientation, or to the value Jamming.

The final outcome function can be computed from the immediate action functions. For a stable orientation f_i, the Jamming intervals in the immediate action function appear as Jamming intervals in its final outcome function. The Non-action intervals map onto index i. The Passing intervals map onto index i-1 (or $n + i$-1 if i-1 $\leq$ 0). The Repeating intervals map onto index i-1, or must be further subdivided by considering the immediate action function of the next stable orientation. This has to be repeated until either all intervals are filled in, or we cyclically reach f_i again, in which case the remaining intervals are labeled jamming (because the part will keep on rotating in front of the pin). See Figure 9 for an example.

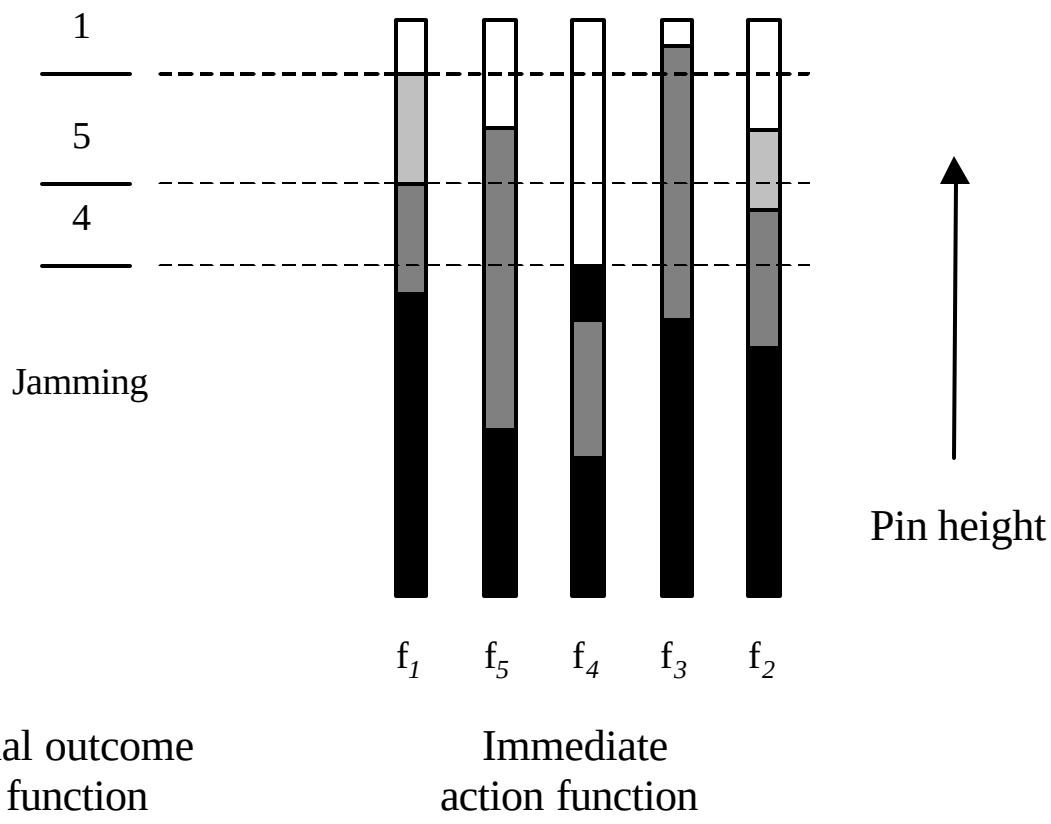

Figure 9. Pin action diagram: the computation of the final outcome function for stable orientation f_1 from the immediate action functions. The black vertical bars correspond to Jamming; the heavy shaded bars to Repeating; the light shaded bars to Passing; and the white bars to Non-action.

Because every interval boundary is a boundary in one of the immediate action functions, the complexity of the final outcome function is $O(n^2)$. We need such a function for each of the $O(n)$ stable orientations.

The final outcome function provides the basis for our pin planning algorithm. Initially the part can be at any stable orientation. After passing a pin the part can still lie on a subset of the stable orientations. Clearly, the height of the pin should be such that it never jams the part. So,

it must lie outside of the union of the jamming intervals of all final outcome functions. By merging the final outcome functions, we derive $O(n^3)$ different intervals of pin heights which each maps our set of all possible stable orientations onto (smaller) sets of stable orientations.

For each of the smaller sets we repeat the process of merging the final outcome functions, to compute height intervals for the second pin together with the corresponding, again smaller, sets of stable orientations. We continue until we reach a set of cardinality one (or sets can no longer be reduced). In this way we can compute the smallest set of pins required to uniquely orient the part.

It is easy to see that this algorithm can take exponential time, $O(n^{3n})$, in the worst-case, but we expect it to behave much better in practice. We are currently working to identify properties of the action functions that will allow us to give a faster algorithm to compute pin plans.

VII. Discussion and Future Work

This paper introduces several new functions that comprise the toppling graph and shows how this graph can be used to find critical pin heights for part feeding. We then show how the graph can be used to design sequences of pins.

The critical pin height analysis can be simplified if friction with the conveyor belt is infinite and friction with the pin is zero; this could be accomplished with high friction belts and by designing pins with freely rotating bearings. This would shrink the $P_1P_2P_3$ triangle to a line segment with the pivot point as the critical point. This also merges $H_i(\boldsymbol{q})$ and $J_i(\boldsymbol{q})$ into a single continuous function. $H_i(\boldsymbol{q})$ would be minimized in all cases and the increase in $J_i(\boldsymbol{q})$ due to the increase in conveyor friction would generally be balanced by the decreased ability of the pin to cause jamming. This system in general has the greatest chance of being able to topple the part.

Another practical consideration is that a part in some orientations may not be able to be toppled. In such a case a simple angled wiper that eliminates part orientations above a certain height could reduce the set of orientations to only those that can be reoriented to a single orientation. Finally, another orienting device such as steps[22] or ramps that rotate the part forward- could be used in conjunction with fixed pins.

We are currently applying a variant of this analysis to the design of parallel-jaw grippers[25].

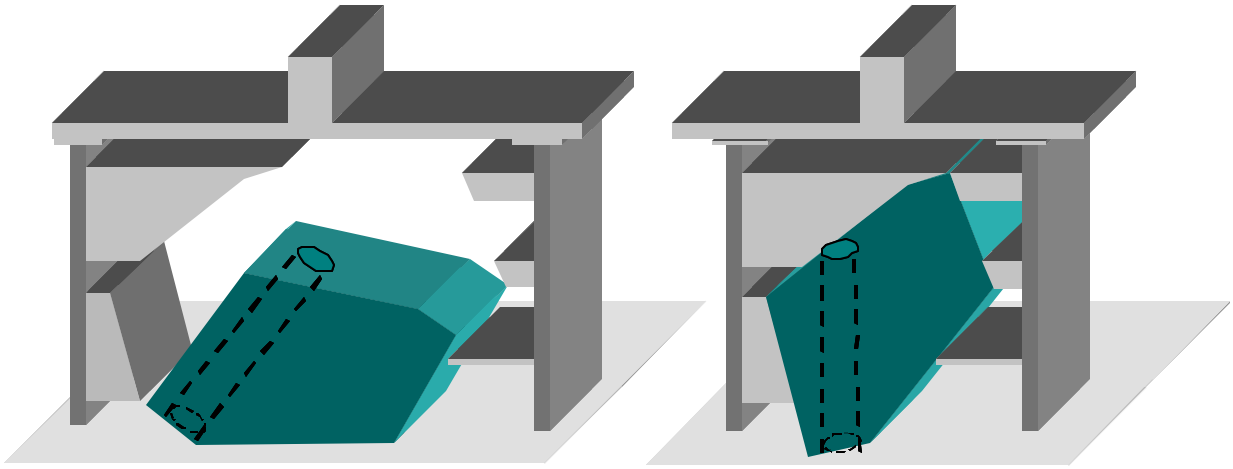

Figure 10. A parallel-jaw gripper compensates for the resting and the desired orientation of a part by toppling during grasping.

ACKNOWLEDGEMENTS

This work was supported in part by NATO Collaborative Research Grant CRG 951224, the National Science Foundation under CDA-9726389 and Presidential Faculty Fellow Award IRI-9553197. Berretty's research is supported by the Dutch Organization for Scientific Research (N.W.O.). We also would like to thank Kevin Lynch for his elegant toppling analysis and ongoing feedback.

REFERENCES

[1] K. Lynch. Toppling Manipulation. In *IEEE International Conference on Robotics and Automation*, Detroit, MI, May 1999.

[2] K. Lynch. Inexpensive Conveyor-Based Parts Feeding. *Assembly Automation*, Vol. 19, No. 3, 1999.

[3] M. A. Erdmann and M. T. Mason. An Exploration of Sensorless Manipulation. *IEEE Journal of Robotics and Automation,* Vol. 4, No. 4, August, 1988.

[4] R. C. Brost. Dynamic Analysis of Planar Manipulation Tasks. In *IEEE International Conference on Robotics and Automation*, Nice, France, May 1992.

[5] K. Goldberg. Orienting polygonal parts without sensors. *Algorithmica*, 10(2):201-225, August, 1993. Special Issue on Computational Robotics.

[6] T. Abell and M. Erdmann. Stably Supported Rotations of a Planar Polygon with Two Frictionless Contacts. In *IEEE/RSJ International Conference on Intelligent Robots and Systems*, Pittsburgh, PA, August 1995.

[7] N. Zumel and M. Erdmann. Nonprehensile Two Palm Manipulation with Non-Equilibrium Transitions between Stable States. In *IEEE International Conference on Robotics and Automation*, Minneapolis, MN, April 1996.

[8] N. Zumel and M. Erdmann. Nonprehensile Manipulation for Orienting Parts in the Plane. In *IEEE International Conference on Robotics and Automation*, Albuquerque, NM, April 1997.

[9] T. Lozano-Perez. Motion Planning and the Design of Orienting Devices for Vibratory Part Feeders. MIT AI Lab Technical Report. January, 1986.

[10] B. K. Natarajan. Some Paradigms for the Automated Design of Part Feeders. *International Journal of Robotics Research*, Vol. 8, No. 6, December, 1989.

[11] M. Caine. The Design of Shape Interactions Using Motion Constraints. In *IEEE International Conference on Intelligent Robots and Systems*, pp. 366-71, 1994.

[12] A. Christiansen, A. D. Edwards, and C. A. C. Coello. Automated Design of Part Feeders Using a Genetic Algorithm. In *IEEE International Conference on Robotics and Automation*, Minneapolis, MN, April, 1996.

[13] D. R. Berkowitz and J. Canny. Designing Parts Feeders Using Dynamic Simulation. In *IEEE International Conference on Robotics and Automation*, Minneapolis, MN, April, 1996.

[14] M. A. Peshkin and A. C. Sanderson. Planning robotic manipulation strategies for workpieces that slide. *IEEE Journal of Robotics and Automation*, 4(5), October, 1998.

[15] J. Wiegley, K. Goldberg, M. Peshkin, and M. Brokowski. A Complete Algorithm for Designing Passive Fences to Orient Parts. In *IEEE International Conference on Robotics and Automation*, pages 550-556, 1998.

[16] R-P Berretty, K. Goldberg, M. H. Overmars, and A. F. Stappen. On Fence Design and the Complexity of Push Plans for Orienting Parts. In *13th ACM Symposium on Computational Geometry*, June, 1997.

[17] D. Gudmundsson and K. Goldberg. Tuning Robotic Part Feeder Parameters to Maximize Throughput. *Assembly Automation*, Vol. 19, No. 3, 1999.

[18] S. Akella, W. Huang, K. Lynch, and M. Mason. "Parts feeding on a conveyor with a one joint robot," *Algorithmica*, Vol.26, No.3-4, pp. 313-344, 2000.

[19] A. Bicchi and R. Sorrentino. Dexterous Manipulation through Rolling. In *IEEE International Conference on Robotics and Automation*, pages 452-457, 1995.

[20] R.-P. Berretty, K. Goldberg, L. Cheung, M. Overmars, G. Smith, and A. Stappen. Trap Design for Vibratory Bowl Feeders. In *IEEE International Conference on Robotics and Automation*, Detroit, MI, May 1999.

[21] S. Blind, C. McCullough, S. Akella, and J. Ponce. "A Reconfigurable Parts Feeder with an Array of Pin," In *IEEE International Conference on Robotics and Automation*, San Francisco, 2000, pp. 147-153.

[22] R. Zhang and K. Gupta. Automatic Orienting of Polyhedral through Step Devices. In *IEEE International Conference on Robotics and Automation*, pages 550-556, 1998.

[23] Y. Yu, K. Fukuda and S. Tsujio. Estimation of Mass and Center of Mass of Graspless and Shape-Unknown Object. In *IEEE International Conference on Robotics and Automation*, Detroit, MI, May 1999.

[24] M. T. Mason. Two Graphical Methods for Planar Contact Problems. In *IEEE/RSJ International Workshop on Intelligent Robots and Systems*, Pages 443-448, Osaka, Japan, November, 1991.

[25] T. Zhang, G. Smith and K. Goldberg. Compensatory Grasping with the Parallel Jaw Gripper. In *4th International Workshop on Algorithmic Foundations of Robotics*, Hanover, NH, March, 2000.